J Biomol NMR (2013) 55:19–31
DOI 10.1007/s10858-012-9675-9

ARTICLE

Utilization of lysine ^{13}C-methylation NMR for protein–protein interaction studies

Yoshikazu Hattori · Kyoko Furuita · Izuru Ohki · Takahisa Ikegami · Harumi Fukada · Masahiro Shirakawa · Toshimichi Fujiwara · Chojiro Kojima

Received: 8 July 2012 / Accepted: 10 September 2012 / Published online: 6 December 2012

Abstract Chemical modification is an easy way for stable isotope labeling of non-labeled proteins. The reductive ^{13}C-methylation of the amino group of the lysine side-chain by ^{13}C-formaldehyde is a post-modification and is applicable to most proteins since this chemical modification specifically and quickly proceeds under mild conditions such as 4 °C, pH 6.8, overnight. ^{13}C-methylation has been used for NMR to study the interactions between the methylated proteins and various molecules, such as small ligands, nucleic acids and peptides. Here we applied lysine ^{13}C-methylation NMR to monitor protein–protein interactions. The affinity and the intermolecular interaction sites of methylated ubiquitin with three ubiquitin-interacting proteins were successfully determined using chemical-shift perturbation experiments via the ^{1}H–^{13}C HSQC spectra of the ^{13}C-methylated-lysine methyl groups. The lysine ^{13}C-methylation NMR results also emphasized the importance of the usage of side-chain signals to monitor the intermolecular interaction sites, and was applicable to studying samples with concentrations in the low sub-micromolar range.

Keywords Protein–protein interaction · Methylated lysine · Reductive methylation · Low concentration sample · Dissociation constant K_d

Electronic supplementary material The online version of this article (doi:10.1007/s10858-012-9675-9) contains supplementary material, which is available to authorized users.

Y. Hattori · K. Furuita · T. Ikegami · T. Fujiwara · C. Kojima
Institute for Protein Research, Osaka University, 3-2 Yamadaoka, Suita, Osaka 565-0871, Japan

I. Ohki (✉) · C. Kojima (✉)
Graduate School of Biological Sciences, Nara Institute of Science and Technology (NAIST), 8916-5 Takayama, Ikoma, Nara 630-0192, Japan
e-mail: i-ooki@bs.naist.jp

C. Kojima
e-mail: kojima@protein.osaka-u.ac.jp

H. Fukada
Graduate School of Life and Environmental Sciences, Osaka Prefecture University, 1-1 Gakuen-cho, Nakaku, Sakai, Osaka 599-8531, Japan

M. Shirakawa
Graduate School of Engineering, Kyoto University, Katsura, Nishikyo-ku, Kyoto 606-8501, Japan

Introduction

Protein–protein interactions play a key role to express cellular functions through enzymatic reactions, signal transductions, and so on. The determination of the protein–protein interaction sites at atomic resolution is an important issue to understand biological processes and to regulate protein functions, and for future drug discovery. NMR spectroscopy is a unique method to determine the protein–protein interaction sites at atomic resolution under physiological conditions (Zuiderweg 2002).

Stable isotope labeling is commonly used for modern protein NMR experiments, such as triple resonance experiments. An *Escherichia coli* expression system can be used to prepare isotopically labeled proteins; however, difficulties may be encountered in obtaining sufficient protein expression, maintaining protein solubility and functional structure. In recent years, isotope labeling techniques using prokaryotic cells, eukaryotic cells or a cell-free system have become available (Kigawa et al. 1995; Takahashi and Shimada 2010). These techniques are also becoming applicable to membrane proteins and larger proteins. However, more difficult targets, such as glycoproteins and extracellular proteins/domains,

remain to be studied using this technique. On the contrary, chemical modification techniques are not plagued by these problems, and can be used for all proteins since purified non-labeled proteins are used for isotope labeling (Bokoch et al. 2010; Religa et al. 2011; Liu et al. 2012).

A mild reaction producing small adducts is preferred for chemical modification of proteins to avoid structural changes. Both reductive methylation of a lysine amino group utilized to incorporate ^{13}C (Jentoft and Dearborn 1983; Bokoch et al. 2010) and modifications of a cysteine thiol group utilized to incorporate ^{13}C and/or ^{19}F (Religa et al. 2011; Liu et al. 2012) meet this criteria. Since lysine is more abundant than cysteine in terms of its frequency in an overall protein and on the protein–protein interface (Chakrabarti and Janin 2002), lysine methylation seems to be the better method to determine the protein–protein interaction sites.

Lysine methylation has been applied to the NMR analyses of the interactions between proteins and metals (Sherry and Teherani 1983; Gerken 1984; Dick et al. 1989; Zhang and Vogel 1993; Abraham et al. 2008), small ligands (Brown and Bradbury 1975; Jentoft et al. 1979; Abraham et al. 2008, 2009; Bokoch et al. 2010), nucleic acids (Dick et al. 1988) and peptides (Zhang and Vogel 1993; Abraham et al. 2008). For the study of protein–protein interactions, only one report exists on the interactions between cytochrome *c* and cytochrome b_5/cytochrome *c* peroxidase (Moore et al. 1998). In these studies, the methylated-lysine methyl groups are assigned on the basis of pK_a values (Brown and Bradbury 1975; Jentoft et al. 1979; Gerken 1984; Dick et al. 1988) and paramagnetic shifts (Sherry and Teherani 1983; Dick et al. 1989; Moore et al. 1998), but these assignments are tentative and partial. On the other hand, the assignments given by mutants are reliable (Zhang and Vogel 1993; Moore et al. 1998; Abraham et al. 2009; Bokoch et al. 2010), and this method has been shown to be applicable to the complete assignments of the methylated-lysine methyl groups of methylated calmodulin (Zhang and Vogel 1993; Abraham et al. 2009). Since complete assignments have not been available except for calmodulin, the utility of the lysine ^{13}C-methylation NMR method to monitor the protein–protein interaction is unclear.

In this study, the resonances of all methyl groups of the methylated-lysine residues were assigned for methylated ubiquitin, and the chemical shift perturbations upon the binding of three interacting proteins were analyzed to determine the protein–protein interaction sites and the binding affinity. YUH1, Dsk2 and p62 were selected as the ubiquitin interacting proteins. YUH1 is a yeast ubiquitin C-terminal hydrolase, and yeast Dsk2 and mouse p62 are ubiquitin binding proteins containing the ubiquitin-associated (UBA) domain (Funakoshi et al. 2002; Ciani et al. 2003). We also evaluated the effect of the methylation on the affinity and the binding sites in the protein–protein interactions.

Materials and methods

Protein preparation

Uniformly ^{15}N-labeled human ubiquitin with an N-terminal glutathione S-transferase (GST)-tag was expressed in *E. coli* Rosetta (DE3) grown in M9 minimum medium containing ^{15}N-ammonium chloride (0.5 g/l) as a sole nitrogen source. Cells were grown at 37 °C to 0.6 A_{600}, then protein expression was induced by isopropyl-β-D-thiogalactopyranoside (IPTG) at a final concentration of 0.5 mM for 4 h at 37 °C. The cultured cells were lysed by sonication and centrifuged. The supernatant was loaded onto the affinity column containing glutathione-Sepharose 4B (GE Healthcare). The protein was eluted with a buffer containing glutathione, and HRV3C protease was added to the eluted solution to cleave the fusion protein. Then, to remove the GST-tag and other impurities, the solution was applied to the gel filtration column containing HiLoad 26/60 Superdex 75 pg (GE Healthcare). Lysine mutants of ubiquitin (K6R, K11R, K27R, K29R, K33R, K48R and K63R) were expressed and purified in the same way.

YUH1 with a C-terminal hexahistidine-tag was expressed in *E. coli* Rosetta (DE3) strain grown in LB medium. Cells were grown at 37 °C to an A_{600} of 0.6, and then protein expression was induced by IPTG at a final concentration of 0.5 mM for 4 h at 37 °C. The cultured cells were lysed by sonication and centrifuged. The supernatant was loaded onto an affinity column containing Ni–NTA Agarose (QIAGEN). The eluate was applied to a gel filtration column containing HiLoad 26/60 Superdex 200 pg (GE Healthcare). The UBA domain of yeast Dsk2 328–373 ($Dsk2_{UBA}$) was prepared as previously reported (Ohno et al. 2005). Briefly, the supernatant was loaded onto the affinity column. The protein was eluted, and thrombin protease was added to remove the GST-tag. Then it was loaded onto an affinity column containing Benzamidine Sepharose 6B (GE Healthcare) to remove the protease, and the eluate was applied to a gel filtration column containing HiLoad 26/60 Superdex 75 pg (GE Healthcare). The UBA domain of mouse p62 391–438 ($p62_{UBA}$) was produced as previously described (Isogai et al. 2011).

Lysine methylation

The amino groups of ubiquitin were methylated by using a protocol based on a previously published method (Rayment 1997). A total of 0.5 ml of 0.1 mM ubiquitin was prepared in a buffer containing 30 mM sodium phosphate (pH 6.8). 10 µl of 1 M dimethylamine borane (Wako Pure Chemical

Industries) was added to the ubiquitin solution, followed by the addition of 40 µl of 1 M ^{13}C-labeled formaldehyde (Cambridge Isotope Lab). The obtained mixture was incubated for 2 h at 4 °C. This step was repeated twice. Then 5 µl of 1 M dimethylamine borane was added and incubated overnight at 4 °C. The reaction was quenched by the addition of 160 µl of 1 M Tris–HCl (pH 8.0), which is 2 molar equivalent to formaldehyde. Finally it was dialyzed to remove the reagents. The amino groups of the ubiquitin mutants were methylated in the same way.

Ubiquitin with the N-terminal GST-tag was methylated for the assignment of the N-terminal methyl groups of ubiquitin. The reaction protocol was the same as above except that the added volume of 1 M ^{13}C-labeled formaldehyde was 300 µl (2 portions of 150 µl) instead of 40 µl. The reaction was quenched by the addition of 600 µl of 1 M Tris–HCl (pH 8.0), and HRV3C protease was added to the reactant to cleave the GST-tag. Then it was applied to the gel filtration column packed with HiLoad 26/60 Superdex 75 pg (GE Healthcare).

NMR samples and measurements

NMR samples were prepared in 275 µl of 95 %/5 % H_2O/D_2O containing 30 mM sodium phosphate (pH 6.8) in 5 mm microtubes (Shigemi). For the experiments with low protein concentrations, samples were prepared in 99.96 % D_2O containing 10 mM sodium phosphate (pH 6.8). NMR measurements were performed at 303 K on 500, 800 and 950 MHz NMR spectrometers equipped with ^{1}H/^{13}C/^{15}N cryogenic probes, and on 400 and 500 MHz machines with ^{1}H/X and ^{1}H/^{13}C/^{15}N normal probes, respectively (Bruker Biospin).

Two-dimensional (2D) ^{1}H–^{13}C correlation spectra were acquired for methylated ubiquitin using a HSQC pulse sequence with gradient enhanced sensitivity improvement (Kay et al. 1992). The ^{13}C t_1 increments were 64–128 points for 10–20 ppm spectral width centered at 45.7 ppm. The scan number was set to 8 or 16 for each FID, and the total experimental time was within 1 h unless otherwise noted. For the titration experiments, the 500 MHz NMR spectrometer was used. For low concentration samples, a 950 MHz NMR spectrometer with cryogenic probe was used with the following parameters. ^{13}C t_1 increments were set to 32 points and extended to 64 points by linear prediction for 10.5 ppm spectral width, which corresponds to 2,500 Hz for the 950 MHz NMR spectrometer. The scan numbers were set to 256 and 1024 for each FID for the free and YUH1 bound forms, and the total experimental times were 2 h 35 min and 10 h 20 min, respectively.

2D ^{1}H–^{15}N correlation spectra for ubiquitin and methylated ubiquitin were acquired using a FHSQC pulse sequence with WATERGATE (Mori et al. 1995). The backbone sequential assignments of ubiquitin and methylated ubiquitin were achieved using 3D HNCA, HN(CO)CA, HN(CA)CB, and HN(COCA)CB spectra (Sattler et al. 1999; Cavanagh et al. 2007) with non-linear sampling procedure. For the YUH1 bound form, the reported assignments (Sakamoto et al. 1999) were used. For the other bound forms, the assignments were achieved by tracing the titration shifts.

The acquired data were processed and analyzed by NMRPipe (Delaglio et al. 1995) and Sparky (Goddard and Kneller 1999), respectively. ^{1}H chemical shifts were referenced to 2,2-dimethyl-2-silapentane-5-sulfonic acid (DSS), and ^{13}C chemical shifts were indirectly referenced to DSS using the ^{1}H/^{13}C gyro magnetic ratios (Wishart et al. 1995). The weighed averages of ^{15}N and ^{1}H chemical shift differences ($\Delta\delta_{H+N}$) were calculated by the equation $\Delta\delta_{H+N} = (\delta_H^2 + (\delta_N/5)^2)^{1/2}$, where δ_H and δ_N represent the differences in ^{1}H and ^{15}N chemical shifts (ppm), respectively.

The assignments of methylated-lysine methyl groups of methylated ubiquitin were performed using mutants (K6R, K11R, K27R, K29R, K33R, K48R and K63R). For the bound form, the assignments were performed by tracing peak shifts through the titration. For K11, the methyl groups showed untraceable changes upon YUH1 binding, thus the assignment was performed using the K11R mutant.

NMR titration experiments

For the titration experiment with YUH1, the initial concentration of methylated ubiquitin was set to 0.05 mM, and 0.74 mM YUH1 was added to methylated ubiquitin at molar ratios of 0.20, 0.40, 0.80, 1.2, 2.0 and 4.0. For $Dsk2_{UBA}$, the initial concentration of methylated ubiquitin was set to 0.10 mM, and 0.93 mM $Dsk2_{UBA}$ was added to methylated ubiquitin at molar ratios of 0.18, 0.45, 0.88, 1.3, 2.2 and 4.0. For $p62_{UBA}$, the initial concentration of methylated ubiquitin was set to 0.10 mM, and 1.38 mM $p62_{UBA}$ was added to methylated ubiquitin at molar ratios of 0.18, 0.46, 0.92, 1.8, 3.5 and 5.5.

Dissociation constants (K_d) were calculated by the non-linear least square method, where 1:1 binding stoichiometry was assumed. The peaks showing titration shifts larger than half of the line width ($\sim$3 Hz) were used in the calculation. Error for the K_d value was estimated by a Monte Carlo procedure. Experimental peak-position and the spectral digital resolution were assumed to be the mean and standard deviation of a Gaussian distribution, respectively. From each such distribution, 50 synthetic peak-position data sets were created. The K_d value was calculated for each of the 50 synthetic peak-position data sets. The standard deviation of the resulting ensemble of the K_d value was taken as the estimated error.

Isothermal titration calorimetry (ITC) experiments

Before the ITC experiments, purified samples were dialyzed against 30 mM sodium phosphate (pH 6.8) and 100 mM NaCl. This dialysis buffer was used to measure heats of dilution. ITC experiments were performed at 298 K using an Omega Micro Calorimeter (Microcal Inc.). YUH1 (0.62 mM) was titrated 28 times every 5 min by adding 10 µl into 49 µM ubiquitin or 54 µM methylated ubiquitin. The experimental data were analyzed using the Origin-ITC software package (OriginLab). Heats of dilution were subtracted from the raw data before analysis.

Results

NMR spectrum of methylated-lysine methyl groups

All amino groups, lysine side-chains and the N-terminus are potential chemical- methylation sites of proteins (Figure S1). Ubiquitin possessing eight amino groups, seven lysine side-chains and one N-terminus, was subjected to chemical-methylation using excess ^{13}C-formaldehyde (200-fold of the reactive site). After the chemical-methylation, the molecular mass increased by 239.9 Da evaluated from the MALDI-MS spectra (Figure S2), and it was identical to the calculated value 240.3 Da assuming two hydrogen atoms were replaced with two $^{13}CH_3$ groups (^{13}C di-methylation) at all eight amino groups, within the error range. In the ^{1}H–^{13}C HSQC spectrum of the methylated ubiquitin (Figure S3a), all methyl peaks of methylated lysine appeared around 45 ppm in the ^{13}C dimension, indicating that all amino groups are di-methylated, since the methyl signals of mono-methylated lysine appear around 35 ppm in the ^{13}C dimension (Jentoft et al. 1979). When less ^{13}C-formaldehyde (tenfold of the reactive site) was used for the chemical-methylation, the reaction was not completed and the methyl peaks appeared around both 35 and 45 ppm in the ^{13}C dimension (Figure S3b). These data indicated that under our experimental condition using 200-fold ^{13}C-formaldehyde, all amino groups of lysine residues and the N-terminus of ubiquitin were fully di-methylated. It should be noted that the fully di-methylated sample makes the required spectral width narrower in the ^{13}C dimension and the resulted experimental time shorter.

The resonance assignment of the methylated-lysine methyl groups of the fully di-methylated ubiquitin, hereinafter called *methylated ubiquitin*, was performed generating a point mutation of each lysine to arginine, and digesting the N-terminal GST-tag of the methylated GST-ubiquitin fusion protein (Fig. 1). From the spectra of the mutants and the digested product, it was evident that peaks

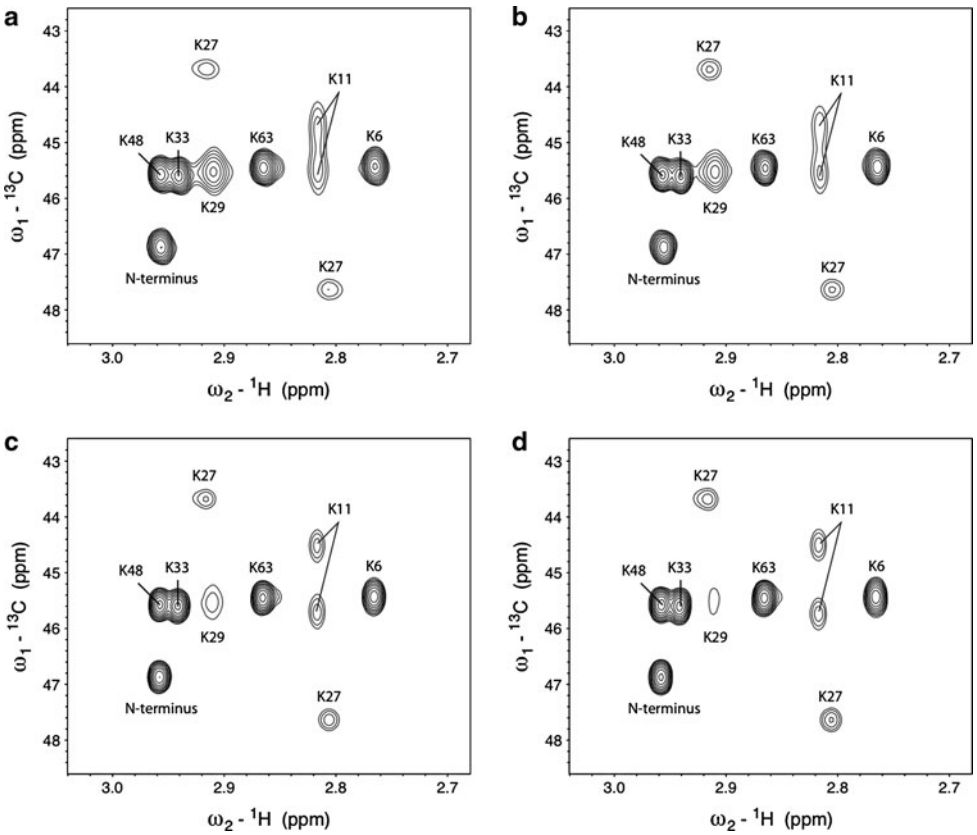

Fig. 1 ^{1}H–^{13}C HSQC spectra of *methylated ubiquitin* and its resonance assignment. K11 and K27 give two peaks owing to slow exchange. The NMR spectra are acquired at **a** 400 MHz, **b** 500 MHz, **c** 800 MHz and **d** 950 MHz

had disappeared without obvious shifts of other peaks (Figure S4). Under our experimental condition, the line shape was different to each other especially in the ^{13}C dimension. After changing the magnetic field from 400 to 950 MHz, it was found that K27 was in slow exchange on the NMR time scale, K11 was in slow to intermediate exchange, K29 was in intermediate to fast exchange, and all others were in fast exchange (Fig. 1). An apparent correlation was observed between these line shape differences and the reported generalized order parameters, S^2, of the lysine amino groups of ubiquitin (Esadze et al. 2011). That is, K27 showed the largest S^2 value (0.71) on the lysine amino group and slow exchange on the ^{13}C methylated-lysine methyl groups, K11 and K29 showed the larger S^2 values (0.42 and 0.38, respectively) and intermediate exchange, and the others showed the smaller S^2 values (less than 0.3) and fast exchange.

The reason for slowing the exchange rate between the two methyl groups of the di-methylated lysine is the formation of a salt bridge (Gerken et al. 1982; Sherry and Teherani 1983; Bokoch et al. 2010). Indeed, for K11 and K27, the average distances between the lysine N^{ζ} and the carboxyl oxygens were within the salt-bridge distance ($\leq$4 Å) (Kumar and Nussinov 2002) in the crystal structure of non-methylated ubiquitin (Vijaykumar et al. 1987). For K29, the lysine side chain did not form the salt bridge, but the distance between the lysine N^{ζ} and backbone carbonyl oxygen was within the hydrogen-bond distance ($\leq$3.5 Å) (Baker and Hubbard 1984), and the *J*-coupling between $^{15}N^{\zeta}$ and carbonyl ^{13}C nuclei across the hydrogen bond were observed (Zandarashvili et al. 2011).

Ubiquitin-YUH1 interaction

ITC experiments were performed to evaluate the effect of the methylation on protein–protein interactions. Either of non-methylated ubiquitin and *methylated ubiquitin* was titrated into YUH1. The dissociation constants (K_d) of YUH1 with non-methylated ubiquitin and *methylated ubiquitin* were determined to be 9.4 ± 0.3 and 5.7 ± 0.1 μM, respectively (Figure S5 and Table S1). The K_d value of *methylated ubiquitin* was smaller than the value of non- methylated ubiquitin. However, the binding mode was considered to be quite similar, since ΔH and ΔS values of non-methylated ubiquitin and *methylated ubiquitin* are in very good agreement with each other (Table S1). To confirm this assumption, the conventional ^{1}H and ^{15}N chemical shift perturbation experiments were performed for non-methylated ubiquitin and *methylated ubiquitin* using ^{1}H–^{15}N HSQC spectra (Figure S6a). The chemical shift changes of the backbone amide groups were well correlated between non-methylated ubiquitin and *methylated ubiquitin* (Figure S6b). These ITC and NMR data suggest that in this system, the binding interface does not change after the methylation.

Using the lysine ^{13}C-methylation NMR, the chemical shift perturbation experiment was applied to monitor the interaction between *methylated ubiquitin* and YUH1 (Fig. 2a). ^{1}H–^{13}C HSQC spectra of the ^{13}C methylated-lysine methyl groups were measured (Fig. 2a), and ^{1}H chemical shift changes were used for further analyses. For split peaks, the averaged chemical shift value was used to show the chemical shift change. K6, K11, K27 and K48 showed significant ^{1}H chemical shift changes $\geq$0.01 ppm (Fig. 2b). All amino groups of these residues were located on the binding interface between ubiquitin and YUH1 in the crystal structure of the complex (Johnston et al. 1999). The binding interface was judged by the intermolecular distance, within 6 Å (Ofran and Rost 2003) (Fig. 2c). All ^{1}H chemical shift changes except for K11 were used for the K_d value determination. K11 was in slow to intermediate exchange and the titration curve was not obtained (Figure S7). Fitting 4 titration curves simultaneously, the K_d value was determined to be 5.6 ± 1.3 μM assuming 1:1 binding stoichiometry (Fig. 2d), and consistent with the value 5.7 ± 0.1 μM determined by the ITC experiment (Table S1).

NMR titration experiment using $Dsk2_{UBA}$

The chemical shift perturbation experiment was applied to monitor the interaction between *methylated ubiquitin* and $Dsk2_{UBA}$ using the lysine ^{13}C-methylation NMR (Fig. 3a). K6, K11 and K48 showed significant ^{1}H chemical shift changes $\geq$0.01 ppm in ^{1}H–^{13}C HSQC (Fig. 3b). The amino groups of K6, K11 and K48 were 3.1 ± 1.0, 13.4 ± 0.5 and 5.8 ± 0.7 Å apart from the binding interface between ubiquitin and $Dsk2_{UBA}$ in the NMR structure of the complex (Ohno et al. 2005), respectively. Thus, the amino groups of K6 and K48 were located on the interface, but K11 was not (Fig. 3c). The significant but much smaller shift changes of K11 may be due to the structural change induced by the ubiquitin-$Dsk2_{UBA}$ complex formation; in fact, the root-mean-square deviation (RMSD) values between free ubiquitin and ubiquitin-$Dsk2_{UBA}$ complex structures were larger than 1 Å on the β1–β2 loop where K11 is located. Fitting 5 titration curves simultaneously, the K_d value was determined to be 2.9 ± 1.4 μM assuming 1:1 binding stoichiometry (Fig. 3d). This value was comparable but significantly smaller than the previously reported value of 14.8 ± 5.3 μM determined by the surface plasmon resonance experiment for yeast ubiquitin (Ohno et al. 2005). This difference in the K_d value may be explained by the differences in the experimental conditions such as buffer, salt concentration and pH, and potentially the presence of the methylation.

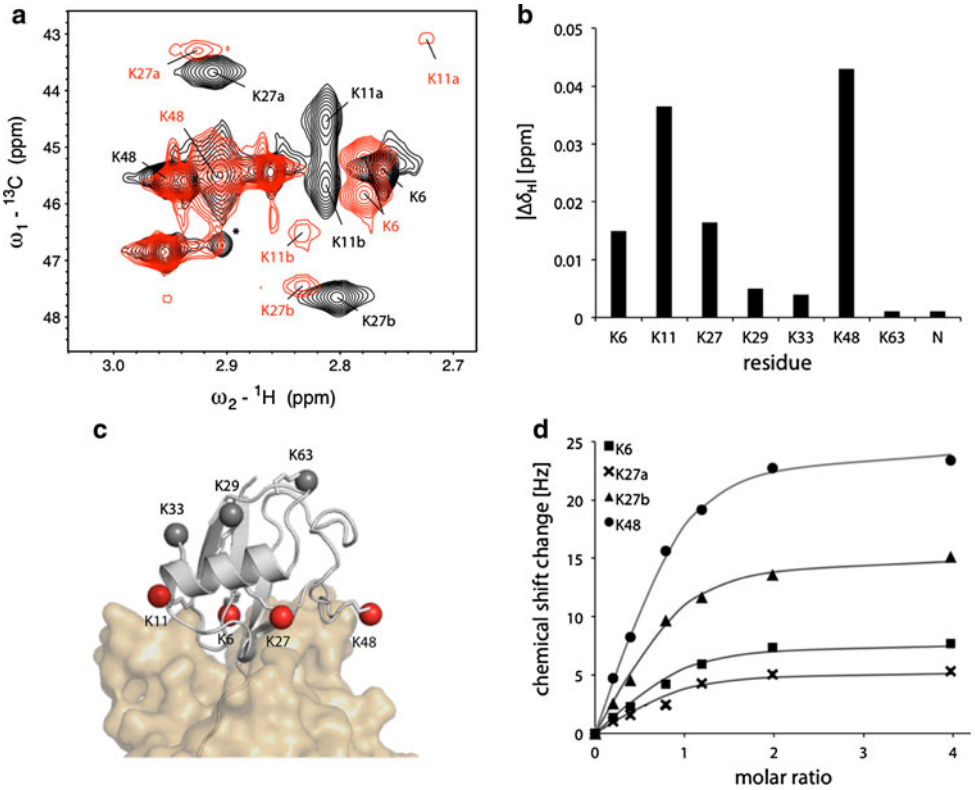

Fig. 2 Titration experiments by lysine ^{13}C-methylation NMR. YUH1 is titrated to *methylated ubiquitin* and monitored by the methylated-lysine methyl groups. **a** The overlay of the ^{1}H–^{13}C HSQC spectra of *methylated ubiquitin* (*black*) and *methylated ubiquitin* with fourfold YUH1 (*red*). *Asterisk* indicates a minor peak from the N-terminus. **b** Absolute values of the ^{1}H chemical shift changes of *methylated ubiquitin* in the presence of YUH1. The chemical shift changes of K11 and K27 are calculated from the averaged chemical shifts of two split peaks, K11a/K11b and K27a/K27b, respectively. **c** Ubiquitin-YUH1 complex structure (PDB ID: 1CMX). Ubiquitin and YUH1 are shown by the ribbon and surface representation, respectively. Lysine N^{ζ} atoms of ubiquitin are shown by *spheres*. Chemical shift changes larger and smaller than 0.01 ppm are *colored red* and *gray*, respectively. **d** Titration curves for K6, K27a, K27b and K48 of *methylated ubiquitin*. Absolute values of the ^{1}H chemical shift changes are shown. The K_d value of *methylated ubiquitin* and YUH1 was 5.6 ± 1.3 μM

NMR titration experiment using $p62_{UBA}$

The chemical shift perturbation experiment was applied to monitor the interaction between *methylated ubiquitin* and $p62_{UBA}$ using the lysine ^{13}C-methylation NMR (Fig. 4a). K6 and K48 showed significant ^{1}H chemical shift changes ≥0.01 ppm in ^{1}H–^{13}C HSQC (Fig. 4b). As shown in Fig. 4c, the $p62_{UBA}$ monomer binds ubiquitin using the same binding mode as with other canonical UBA domains, and the $p62_{UBA}$ dimer does not bind ubiquitin (Isogai et al. 2011). In this modeled structure (Fig. 4c), the amino groups of K6 and K48 were located on the binding interface between ubiquitin and $p62_{UBA}$. Since both $p62_{UBA}$ and $Dsk2_{UBA}$ belong to the canonical UBA domain family, the binding interface of the $p62_{UBA}$ complex is expected to be similar to that of the $Dsk2_{UBA}$ complex. For the $Dsk2_{UBA}$ complex, K6, K11 and K48 showed significant changes ≥0.01 ppm, and K6 and K48 showed the largest and the second largest shifts, respectively (Fig. 3b). This tendency was kept in the $p62_{UBA}$ complex except that the magnitude of the change was much smaller. For example, K11 of the $p62_{UBA}$ complex showed the third largest shifts consistent with the $Dsk2_{UBA}$ complex, but the magnitude was smaller than 0.01 ppm.

In an effort to determine the K_d value between *methylated ubiquitin* and the $p62_{UBA}$ monomer, three titration curves were fitted simultaneously assuming 1:1 binding stoichiometry. However the titration curves did not fit well with using a 1:1 binding mode (Figure S9). It has been reported that the K_d value of $p62_{UBA}$ dimer formation is 3.5 μM (Isogai et al. 2011) and the dimerization is much stronger than ubiquitin binding (Long et al. 2010; Isogai et al. 2011). Thus we assumed the presence of two equilibriums, $K_d = [\text{ubiquitin}][p62_{UBA}]/[\text{ubiquitin} - p62_{UBA}]$ and K_d (dimer) $= [p62_{UBA}]^2/[p62_{UBA} - p62_{UBA}] =$ 3.5 μM, where [ubiquitin], $[p62_{UBA}]$, [ubiquitin-$p62_{UBA}$], and $[p62_{UBA} - p62_{UBA}]$ are the concentration of *methylated ubiquitin*, $p62_{UBA}$, the complex between *methylated ubiquitin* and $p62_{UBA}$ monomer, and $p62_{UBA}$ dimer, respectively. Since the $p62_{UBA}$ dimer does not bind ubiquitin (Long et al.

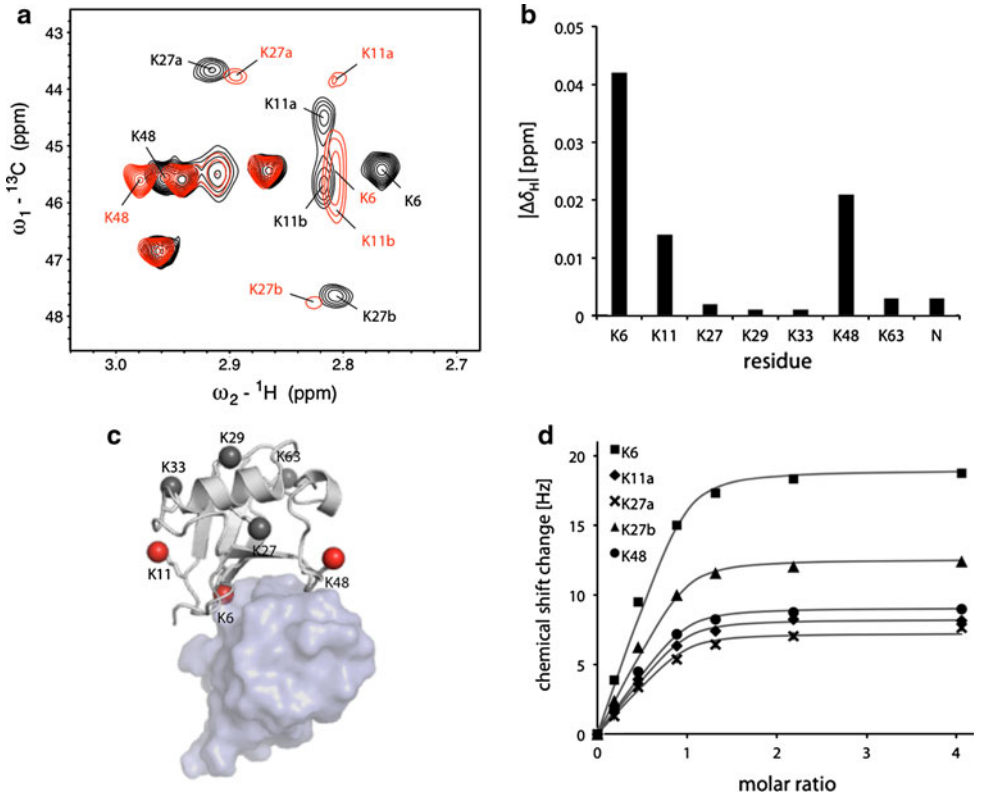

Fig. 3 Titration experiments by lysine ^{13}C-methylation NMR. Dsk2$_{UBA}$ is titrated to *methylated ubiquitin* and monitored by the methylated-lysine methyl groups. **a** The overlay of the ^{1}H–^{13}C HSQC spectra of *methylated ubiquitin* (*black*) and *methylated ubiquitin* with fourfold Dsk2$_{UBA}$ (*red*). *Asterisk* indicates a minor peak from the N-terminus. **b** Absolute values of the ^{1}H chemical shift changes of *methylated ubiquitin* in the presence of Dsk2$_{UBA}$. The chemical shift change of K27 is calculated from the averaged chemical shifts of two split peaks, K27a and K27b. **c** Ubiquitin-Dsk2$_{UBA}$ complex structure (PDB ID: 1WR1). Ubiquitin and Dsk2$_{UBA}$ are shown by the ribbon and surface representation, respectively. Lysine N$^{\zeta}$ atoms of ubiquitin are shown by *spheres*. Chemical shift changes larger and smaller than 0.01 ppm were *colored* by *red* and *gray*, respectively. **d** Titration curves for K6, K11a, K27a, K27b and K48 of *methylated ubiquitin*. Absolute values of the ^{1}H chemical shift changes are shown. The K_d value of *methylated ubiquitin* and Dsk2$_{UBA}$ was 2.9 ± 1.4 μM

2010; Isogai et al. 2011), two equilibriums are enough to describe the whole system. Thus, three titration curves were fitted simultaneously assuming that these two equilibriums exist. The titration curves fitted very well, and the K_d value between *methylated ubiquitin* and the p62$_{UBA}$ monomer was determined to be 24 ± 3 μM (Fig. 4d). This value was comparable to the previously reported values of a few tens of μM (Isogai et al. 2011) and 40 ± 10 μM (Long et al. 2010) determined by NMR experiments. In this two-equilibrium system, the chemical shift perturbation using the lysine ^{13}C-methylation NMR gave the precise K_d value consistent with the reported values, despite the fact that the chemical shift changes were small and the K_d value was large.

Discussion

Side-chain interaction

In the lysine ^{13}C-methylation NMR, the protein–protein interaction is monitored by the chemical shift perturbation of the methyl signals using the ^{1}H–^{13}C HSQC spectra. The introduced methyl groups are located on the terminus of the long side-chain of lysine, apart from the backbone amide group by up to 7 Å. Therefore, the chemical shift perturbation pattern will be somewhat different between the side-chain methyl groups and the backbone amide groups. In an effort to estimate this difference, the chemical shift perturbation experiments of the backbone amide groups of the *methylated ubiquitin* were performed using the ^{1}H–^{15}N HSQC spectra for YUH1, Dsk2$_{UBA}$ and p62$_{UBA}$ (Figure S8), and compared with those of the side-chain methyl groups (Fig. 5).

The chemical shift perturbation pattern was not different for most of the residues between the side-chain methyl groups and the backbone amide groups; however, some significantly large differences were found. Among them, the K6 and K48 residues in Dsk2$_{UBA}$ binding showed the most significant differences (Fig. 5b). The K6 methyl groups showed the largest change among all methyl groups, but the K6 amide group showed the smallest change. This agreed with the result that side-chain amino group of K6 forms a hydrogen bond with the side-chain

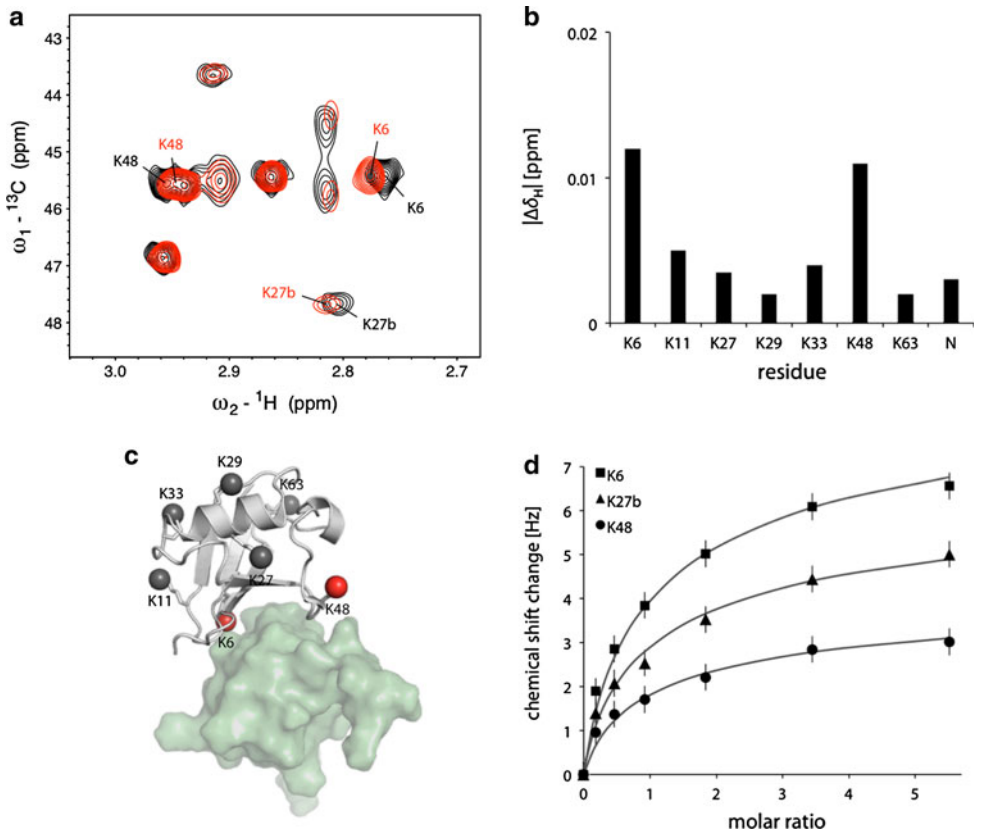

Fig. 4 Titration experiments by lysine ^{13}C-methylation NMR. $p62_{UBA}$ is titrated to *methylated ubiquitin* and monitored by the methylated-lysine methyl groups. **a** The overlay of the ^{1}H–^{13}C HSQC spectra of *methylated ubiquitin* (*black*) and *methylated ubiquitin* with 5.5-fold $p62_{UBA}$ (*red*). *Asterisk* indicates a minor peak from the N-terminus. **b** Absolute values of the ^{1}H chemical shift changes of *methylated ubiquitin* in the presence of $p62_{UBA}$. The chemical shift change of K27 is calculated from the averaged chemical shifts of two split peaks, K27a and K27b. **c** Modeled structure of ubiquitin-$p62_{UBA}$ complex based on the ubiquitin-$Dsk2_{UBA}$ complex structure (PDB ID: 1WR1) and ubiquitin bound form of the $p62_{UBA}$ structure (PDB ID: 2RRU). Ubiquitin and $p62_{UBA}$ are shown by the ribbon and surface representation, respectively. Lysine N^{ζ} atoms of ubiquitin are shown by *spheres*. Chemical shift changes larger and smaller than 0.01 ppm are *colored red* and *gray*, respectively. **d** Titration curves for K6, K27b and K48 of *methylated ubiquitin*. Absolute values of the ^{1}H chemical shift changes are shown. The K_d value of *methylated ubiquitin* and $p62_{UBA}$ was 24 ± 3 μM

carbonyl group of Q338 of $Dsk2_{UBA}$, and the backbone amide group has no such specific interaction (Figs. 5d and S10, Table S2). Similar patterns were found for the changes of K6 and K27 in YUH1 binding, and K6 in $p62_{UBA}$ binding. This agreed with the fact that the side-chain amino groups of K6 and K27 are located on the interface in YUH1 binding, and the backbone amide group is not (Table S2). It is noted that all the lysine residues located on the binding interface show significant chemical shift changes of the methyl groups (≥0.01 ppm), but the half residues do not show significant changes of the backbone amide groups (≥0.2 ppm). That is, for the half residues, the backbone N atoms are not located on the binding interface (Table S2). These data are consistent with the fact that the lysine side-chain amino group tends to locate on the binding interface, but the backbone amide group is removed from the side-chain by up to 7 Å and fails to locate on the binding interface. Therefore, the methylated-lysine methyl groups are good probes to monitor protein–protein interactions, as they are very sensitive to the side-chain interactions which cannot be detected by the backbone amide groups.

Sensitivity

In general, methyl groups give the strongest NMR signals for a protein sample, and the selective labeling of methyl groups is widely used to study large protein complexes (Kay 2011). Thus, the sensitivity of lysine ^{13}C-methylation NMR is expected to be high independent of molecular weight and resonance frequency. To evaluate the sensitivity, lysine ^{13}C-methylation NMR was applied to the 2 and 0.2 μM *methylated ubiquitin* samples to monitor protein–protein interactions using a 950 MHz NMR spectrometer equipped with a cryogenic probe. At 2 μM, all peaks of the methylated-lysine methyl groups were observed (Fig. 6a). In the presence of YUH1, the K29 signal was missing but all other peaks including the shifted peaks of K6, K11, K27 and K48 were detected. At 0.2 μM,

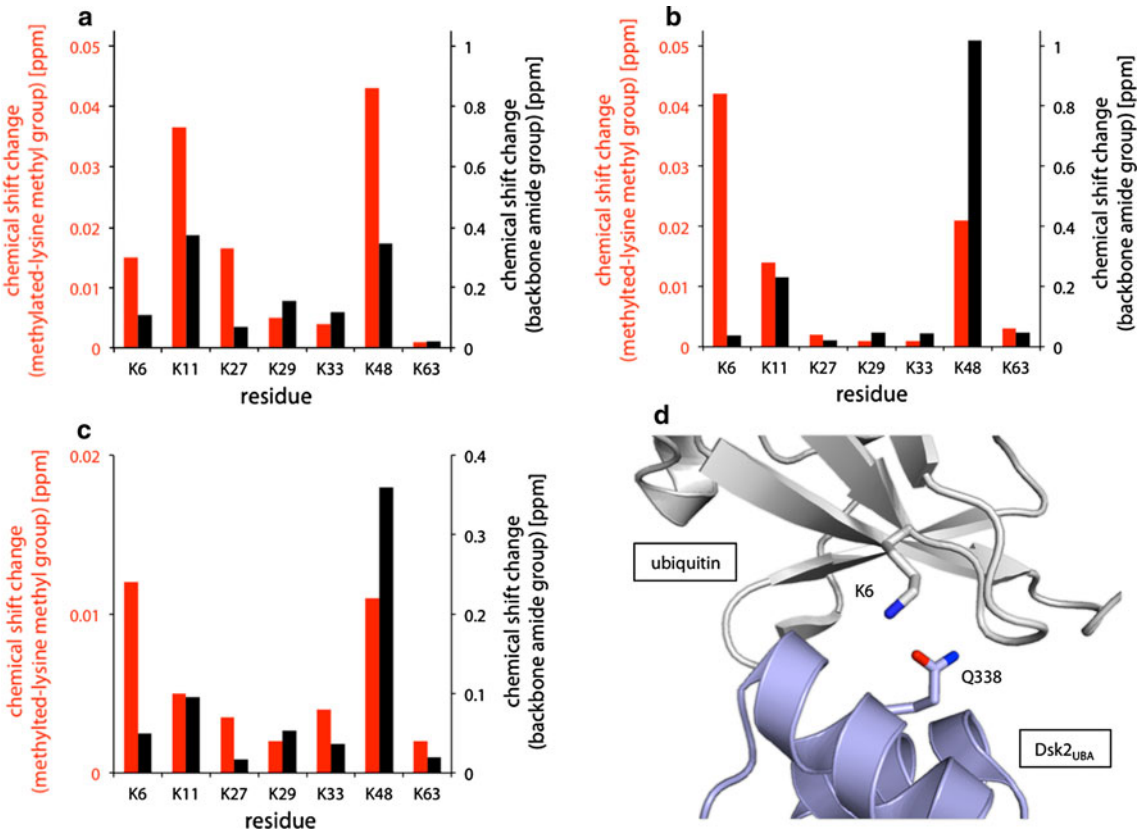

Fig. 5 Chemical shift changes of lysine methyl groups (*red*) and backbone amide groups (*black*) of *methylated ubiquitin* in the presence of **a** YUH1, **b** $Dsk2_{UBA}$ and **c** $p62_{UBA}$. **d** Enlarged view of Fig. 3c, where $Dsk2_{UBA}$ *colored blue* is shown by the ribbon representation instead of surface representation. The side-chains of K6 of ubiquitin and Q338 of $Dsk2_{UBA}$ are shown by the stick representation

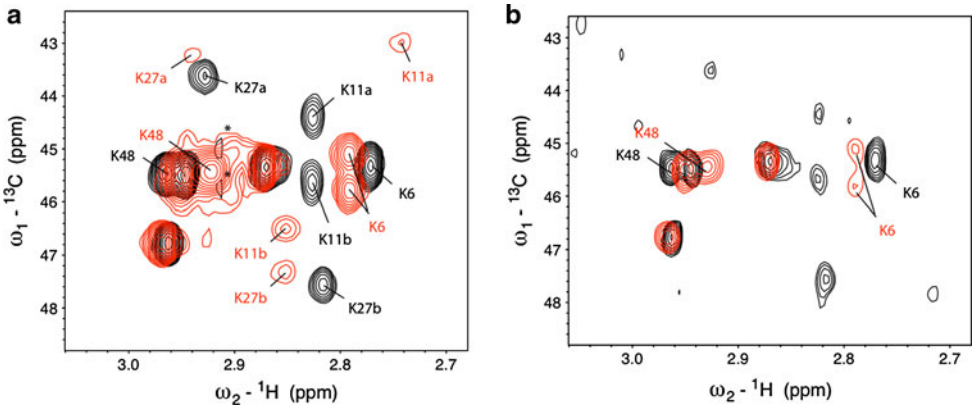

Fig. 6 Titration experiments by lysine ^{13}C-methylation NMR at low concentration. YUH1 is titrated to *methylated ubiquitin* and monitored by the methylated-lysine methyl groups. **a** The overlay of the ^{1}H–^{13}C HSQC spectra of 2 μM *methylated ubiquitin* (*black*) and *methylated ubiquitin* with tenfold YUH1 (*red*). *Asterisk* indicates K29. **b** Same as **a** with 0.2 μM *methylated ubiquitin*. All spectra were recorded on 950 MHz NMR

all peaks of methylated-lysine methyl groups were observed except for K29 (Figs. 6b and S12). In the presence of YUH1, all peaks were observed except for K11, K27 and K29. These missing residues are in slow to intermediate exchange (Fig. 1), and their signal intensities were much weaker than the others even in the free state. In this sense, the resonance frequency affects the sensitivity through the line shape change owing to the exchange process. It is noted that the further sensitivity gain is expected if a straight HSQC/HMQC pulse sequence is used, since the gradient sensitivity enhancement scheme used in this report gives slightly (~20 %) worse S/N ratios than the straight one for CH_3 groups (Figure S11). These data suggest that the sensitivity of lysine ^{13}C-methylation

NMR is very high and applicable to a low concentration sample, at least sub-μM using state-of-the-art NMR hardware to monitor protein–protein interactions.

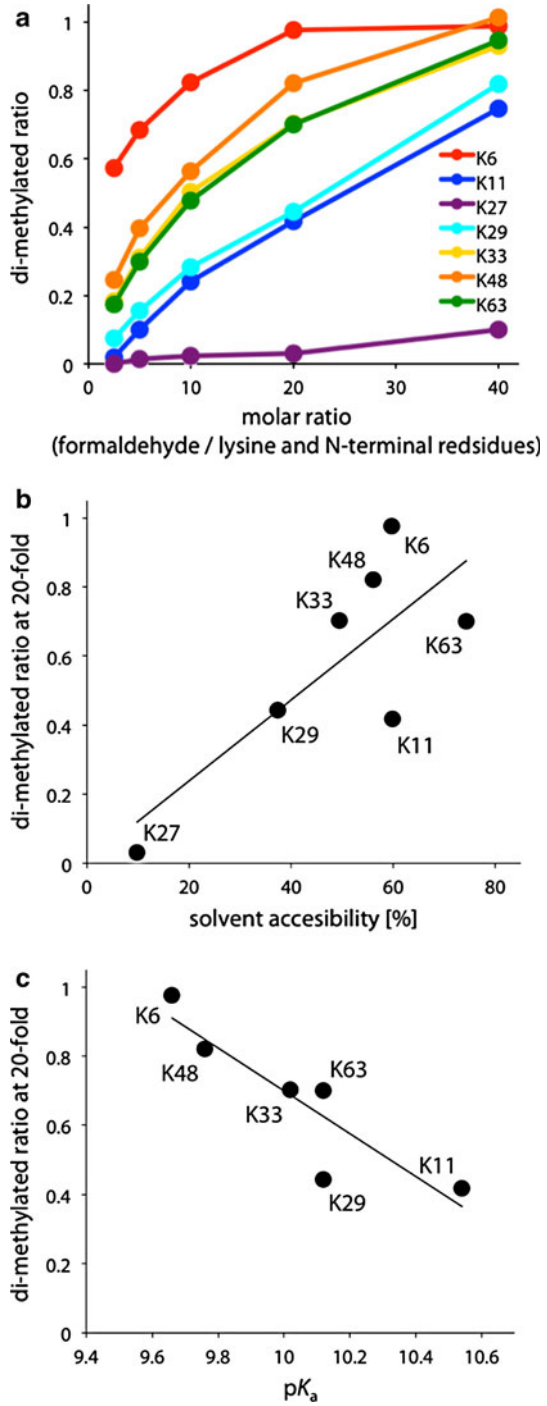

Fig. 7 Reactivity. **a** The di-methylated ratio against the molar ratio of formaldehyde. The di-methylated ratio is estimated from the peak volumes of the ^{13}C-HSQC spectra. **b** The di-methylated ratio at 20-fold formaldehyde against the solvent accessibility. Least square fitted line is shown. **c** Same as **b** against pK_a value. The pK_a value of K27 is not reported

Reactivity

Lysine ^{13}C-methylation NMR is applicable for a wide range of targets because the methylation reaction proceeds at neutral pH and 4 °C. The protein function is expected to be maintained because the methylated lysine maintains a similar pK_a value for the N^{ζ} atom and is protonated at neutral pH (Bradbury and Brown 1973; Jentoft et al. 1979). The lysine methylation also improves the crystallization probability (Rayment 1997; Walter et al. 2006). In this report, the fully di-methylated ubiquitin is prepared by using 200-fold excess formaldehyde. When the amount of the formaldehyde was decreased, the ratio of the di-methylated lysine was decreased drastically (Fig. 7a). The reactivity was obviously different from one residue to another. For example, K6 and K27 were the most and least reactive residues, respectively. When the 40-fold formaldehyde was used instead of 200-fold, most lysine residues were di-methylated but K27 was not. The reactivity depended on the solvent accessibility, and a positive correlation between them was observed (Fig. 7b). The solvent accessibilities were calculated by GetArea (Fraczkiewicz and Braun 1998) using the crystal structure (PDB ID: 1UBQ) and the radius of the water probe was set to 1.4 Å. The least reactive residue K27 showed the smallest solvent accessibility by far. The reactivity also depended on the reported apparent pK_a values (Macdonald et al. 1999), and a negative correlation between them was observed

Table 1 Cα RMSD values of the non-methylated and methylated proteins

UniProt ID	PDB ID (non-methylated)	PDB ID (methylated)	Cα RMSD[a] (Å)
P00698	1LYZ	132L	0.62
O96555	1Z27	1Z1Y	0.72
Q9X0A5	2EWR	2FCL	0.31
Q97PV8	2HO5	2HO3	0.48
Q87IM6	2QM2	2QHQ	0.47
P0AEH1	3ID2	2ZPM	1.05
Q81VF6	3HA1	2VD8	0.27
Q83Q96	2HKT	3C8G	0.25
Q838I6	2IAC	3BED	0.16
P0A7Z4	1LB2	3K4G	0.79
O05510	1XC3	3OHR	0.25
O58035	2ZZF	2ZZE	0.95
Q6NC90	3DCA	3HHL	0.43
P00447	3BFR	3LSU	0.32
A0KF03	3PSZ	3PSS	0.94
P07550	2R4S	3KJ6	0.51

[a] The RMSD values are calculated using FATCAT structural alignments (Ye and Godzik 2003). When the structure is the oligomer, the smallest RMSD value is shown in the list

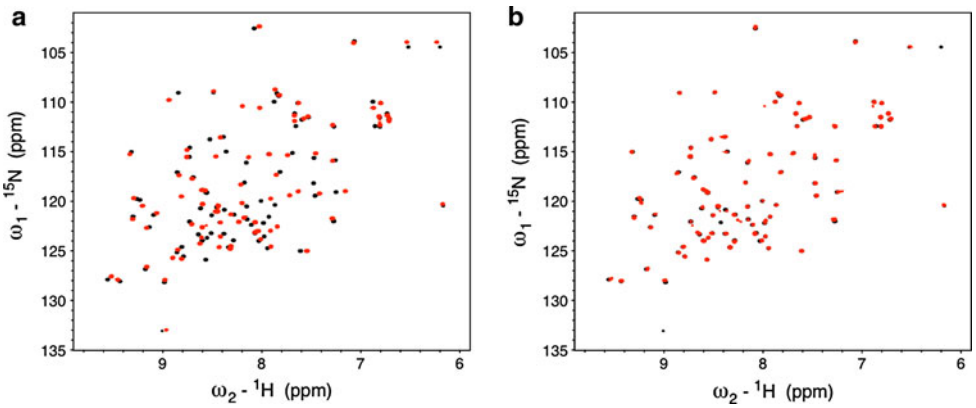

Fig. 8 Overlay of the ^{1}H–^{15}N HSQC spectra of non-methylated ubiquitin (*black*) and *methylated ubiquitin* (*red*). Ubiquitin was methylated using **a** 200-fold or **b** tenfold of ^{13}C-formaldehyde

(Fig. 7c). This relationship is reasonable because the methylation reaction includes the de-protonation of the amino groups (Figure S1).

Structural change induced by lysine methylation

In lysine ^{13}C-methylation NMR, ^{13}C-methyl groups are conjugated to all amino groups of the protein which may result in a structural change of the methylated protein. In an effort to evaluate the potential structural changes induced by the methylation, the protein data bank (www.pdbj.org) was surveyed. More than 100 crystal structures of methylated proteins were found. For 16 proteins, both non-methylated and methylated structures were found, and the RMSD values of the backbone C_α atoms between the non-methylated and methylated structures were calculated (Table 1). The averaged RMSD value was 0.5 ± 0.3 Å, and the maximum RMSD value was 1.05 Å. These numbers indicate that no or little structural change is induced by the lysine methylation.

The structural change induced by the lysine methylation was further studied using NMR. ^{1}H–^{15}N HSQC spectra were measured for non-methylated ubiquitin and *methylated ubiquitin* (Figs. 8a and S13a). Significantly large changes $\geq$0.4 ppm were observed for the residues E24, D39 and G53. These residues were mapped on the ubiquitin structure, and located spatially-close to K27 (Figure S13b). K27 was the most buried residue, and its solvent accessibility was less than 10 %. The methylation of a buried lysine may be more likely to cause a detectable structural change. As described above, the reactivity of K27 was significantly lower than the others. When the amount of formaldehyde was reduced (tenfold of the reactive site), the observed chemical shift changes were suppressed in the ^{1}H–^{15}N HSQC spectra (Fig. 8b). Under this reaction condition, all methyl peaks of di-methylated-lysine methyl groups except for K27 were observed in the ^{1}H–^{13}C HSQC spectrum (Figure S3b). Therefore, using an appropriate amount of formaldehyde, the buried lysine residue can be excluded in the methylation reaction, and the structural change induced by the lysine methylation can be kept at a minimum.

Conclusion

Lysine ^{13}C-methylation NMR was applied for monitoring the protein–protein interactions between ubiquitin and three interacting proteins, YUH1, $Dsk2_{UBA}$, and $p62_{UBA}$. First, lysine methylation causes little or no impact on the structure and the protein–protein interactions as revealed by a data base survey, ITC, and NMR. Second, the methylated-lysine methyl group is a good probe for monitoring protein–protein interactions and for determining the K_d value. In particular, it is a very sensitive technique for monitoring side-chain interactions that cannot be detected by the backbone amide groups. Last, the sensitivity of lysine ^{13}C-methylation NMR is very high, and the protein–protein interactions can be monitored at a sub-μM protein concentration using a state-of-the-art 950 MHz NMR overnight. All features of lysine ^{13}C-methylation NMR are suitable for monitoring protein–protein interactions, and are applicable to non-labeled proteins and large protein complexes.

Acknowledgments We thank M. Yoneyama and H. Kinoshita for sample preparation; S. Isogai and D. Morimoto for the gift of the $p62_{UBA}$ sample; H. Kobayashi and A. Ohno for the gift of the $Dsk2_{UBA}$ expression vector; and J. Tsukamoto, Y. Hara and A. Nakagawa for mass spectroscopy. This work was supported in part by grants from the Ministry of Education, Culture, Sports, Science and Technology (MEXT) through the Target Proteins Research Program, the Global COE Program at NAIST, and Grants-in-Aid for Scientific Research (20370038, 22121515, 23370053, 20770086) to CK and IO.

References

Abraham SJ, Hoheisel S, Gaponenko V (2008) Detection of protein-ligand interactions by NMR using reductive methylation of lysine residues. J Biomol NMR 42:143–148

Abraham SJ, Kobayashi T, Solaro RJ, Gaponenko V (2009) Differences in lysine pKa values may be used to improve NMR signal dispersion in reductively methylated proteins. J Biomol NMR 43:239–246

Baker EN, Hubbard RE (1984) Hydrogen-bonding in globular-proteins. Prog Biophys Mol Biol 44:97–179

Bokoch MP, Zou YZ, Rasmussen SGF, Liu CW, Nygaard R, Rosenbaum DM, Fung JJ, Choi HJ, Thian FS, Kobilka TS, Puglisi JD, Weis WI, Pardo L, Prosser RS, Mueller L, Kobilka BK (2010) Ligand-specific regulation of the extracellular surface of a G-protein-coupled receptor. Nature 463:108–121

Bradbury JH, Brown LR (1973) Determination of dissociation constants of lysine residues of lysozyme by proton-magnetic-resonance spectroscopy. Eur J Biochem 40:565–576

Brown LR, Bradbury JH (1975) Proton-magnetic-resonance studies of lysine residues of ribonuclease-A. Eur J Biochem 54:219–227

Cavanagh J, Fairbrother WJ, Palmer AG, Rance M, Skelton NJ (2007) Protein NMR spectroscopy, 2nd edn. Academic Press, Inc., San Diego

Chakrabarti P, Janin J (2002) Dissecting protein–protein recognition sites. Proteins 47:334–343

Ciani B, Layfield R, Cavey JR, Sheppard PW, Searle MS (2003) Structure of the ubiquitin-associated domain of p62 (SQSTM1) and implications for mutations that cause Paget's disease of bone. J Biol Chem 278:37409–37412

Delaglio F, Grzesiek S, Vuister GW, Zhu G, Pfeifer J, Bax A (1995) NMRPipe—a multidimensional spectral processing system based on unix pipes. J Biomol NMR 6:277–293

Dick LR, Sherry AD, Newkirk MM, Gray DM (1988) Reductive methylation and C-13 NMR-studies of the lysyl residues of fd gene 5 protein—lysine-24, lysine-46 and lysine-69 may be involved in nucleic-acid binding. J Biol Chem 263:18864–18872

Dick LR, Geraldes C, Sherry AD, Gray CW, Gray DM (1989) C-13 NMR of methylated lysines of fd gene-5 protein—evidence for a conformational change involving lysine-24 upon binding of a negatively charged lanthanide chelate. Biochemistry 28:7896–7904

Esadze A, Li DW, Wang TZ, Bruschweiler R, Iwahara J (2011) Dynamics of lysine side-chain amino groups in a protein studied by heteronuclear H-1-N-15 NMR spectroscopy. J Am Chem Soc 133:909–919

Fraczkiewicz R, Braun W (1998) Exact and efficient analytical calculation of the accessible surface areas and their gradients for macromolecules. J Comput Chem 19:319–333

Funakoshi M, Sasaki T, Nishimoto T, Kobayashi H (2002) Budding yeast Dsk2p is a polyubiquitin-binding protein that can interact with the proteasome. Proc Natl Acad Sci USA 99:745–750

Gerken TA (1984) Amino group environments and metal-binding properties of C-13 reductively methylated bovine alpha-lactal-bumin. Biochemistry 23:4688–4697

Gerken TA, Jentoft JE, Jentoft N, Dearborn DG (1982) Intramolecular interactions of amino-groups in C-13 reductively methylated hen egg-white lysozyme. J Biol Chem 257:2894–2900

Goddard TD, Kneller DG (1999) SPARKY3. University of California, San Francisco

Isogai S, Morimoto D, Arita K, Unzai S, Tenno T, Hasegawa J, Sou Y-s, Komatsu M, Tanaka K, Shirakawa M, Tochio H (2011) Crystal structure of the ubiquitin-associated (UBA) domain of p62 and its interaction with ubiquitin. J Biol Chem 286:31864–31874

Jentoft N, Dearborn DG (1983) Protein labeling by reductive alkylation. Method Enzymol 91:570–579

Jentoft JE, Jentoft N, Gerken TA, Dearborn DG (1979) C-13 NMR-studies of ribonuclease-a methylated with formaldehyde-C-13. J Biol Chem 254:4366–4370

Johnston SC, Riddle SM, Cohen RE, Hill CP (1999) Structural basis for the specificity of ubiquitin C-terminal hydrolases. EMBO J 18:3877–3887

Kay LE (2011) Solution NMR spectroscopy of supra-molecular systems, why bother? A methyl-TROSY view. J Magn Reson 210:159–170

Kay LE, Keifer P, Saarinen T (1992) Pure absorption gradient enhanced heteronuclear single quantum correlation spectroscopy with improved sensitivity. J Am Chem Soc 114:10663–10665

Kigawa T, Muto Y, Yokoyama S (1995) Cell-free synthesis and amino acid-selective stable-isotope labeling of proteins for NMR analysis. J Biomol NMR 6:129–134

Kumar S, Nussinov R (2002) Close-range electrostatic interactions in proteins. ChemBioChem 3:604–617

Liu JJ, Horst R, Katritch V, Stevens RC, Wuethrich K (2012) Biased signaling pathways in beta(2)-adrenergic receptor characterized by F-19-NMR. Science 335:1106–1110

Long J, Garner TP, Pandya MJ, Craven CJ, Chen P, Shaw B, Williamson MP, Layfield R, Searle MS (2010) Dimerisation of the UBA domain of p62 inhibits ubiquitin binding and regulates NF-kappa B signalling. J Mol Biol 396:178–194

Macdonald JM, LeBlanc DA, Haas AL, London RE (1999) An NMR analysis of the reaction of ubiquitin with acetyl-1-C-13 aspirin. Biochem Pharmacol 57:1233–1244

Moore GR, Cox MC, Crowe D, Osborne MJ, Rosell FI, Bujons J, Barker PD, Mauk MR, Mauk AG (1998) N-epsilon, N-epsilon-dimethyl-lysine cytochrome c as an NMR probe for lysine involvement in protein–protein complex formation. Biochem J 332:439–449

Mori S, Abeygunawardana C, Johnson MO, Vanzijl PCM (1995) Improved sensitivity of HSQC spectra of exchanging protons at short interscan delays using a new fast HSQC (FHSQC) detection scheme that avoids water saturation. J Magn Reson B 108:94–98

Ofran Y, Rost B (2003) Analysing six types of protein–protein interfaces. J Mol Biol 325:377–387

Ohno A, Jee J, Fujiwara K, Tenno T, Goda N, Tochio H, Kobayashi H, Hiroaki H, Shirakawa M (2005) Structure of the UBA domain of Dsk2p in complex with ubiquitin: molecular determinants for ubiquitin recognition. Structure 13:521–532

Rayment I (1997) Reductive alkylation of lysine residues to alter crystallization properties of proteins. Methods Enzymol 276:171–179

Religa TL, Ruschak AM, Rosenzweig R, Kay LE (2011) Site-directed methyl group labeling as an NMR probe of structure and dynamics in supramolecular protein systems: applications to the proteasome and to the CIpP protease. J Am Chem Soc 133:9063–9068

Sakamoto T, Tanaka T, Ito Y, Rajesh S, Iwamoto-Sugai M, Kodera Y, Tsuchida N, Shibata T, Kohno T (1999) An NMR analysis of ubiquitin recognition by yeast ubiquitin hydrolase: evidence for novel substrate recognition by a cysteine protease. Biochemistry 38:11634–11642

Sattler M, Schleucher J, Griesinger C (1999) Heteronuclear multidimensional NMR experiments for the structure determination of proteins in solution employing pulsed field gradients. Prog Nucl Magn Reson 34:93–158

Sherry AD, Teherani J (1983) Physical studies of C-13-methylated concanavalin-A—pH-induced and Co^{2+}-induced nuclear magnetic-resonance shifts. J Biol Chem 258:8663–8669

Takahashi H, Shimada I (2010) Production of isotopically labeled heterologous proteins in non-*E. coli* prokaryotic and eukaryotic cells. J Biomol NMR 46:3–10

Vijaykumar S, Bugg CE, Cook WJ (1987) Structure of ubiquitin refined at 1.8 Å resolution. J Mol Biol 194:531–544

Walter TS, Meier C, Assenberg R, Au KF, Ren JS, Verma A, Nettleship JE, Owens RJ, Stuart DI, Grimes JM (2006) Lysine methylation as a routine rescue strategy for protein crystallization. Structure 14:1617–1622

Wishart DS, Bigam CG, Yao J, Abildgaard F, Dyson HJ, Oldfield E, Markley JL, Sykes BD (1995) H-1, C-13 and N-15 chemical-shift referencing in biomolecular NMR. J Biomol NMR 6:135–140

Ye Y, Godzik A (2003) Flexible structure alignment by chaining aligned fragment pairs allowing twists. Bioinformatics 19: 246–255

Zandarashvili L, Li DW, Wang TZ, Bruschweiler R, Iwahara J (2011) Signature of mobile hydrogen bonding of lysine side chains from long-range N-15-C-13 scalar J-couplings and computation. J Am Chem Soc 133:9192–9195

Zhang MJ, Vogel HJ (1993) Determination of the side-chain pK(a) values of the lysine residues in calmodulin. J Biol Chem 268:22420–22428

Zuiderweg ERP (2002) Mapping protein–protein interactions in solution by NMR spectroscopy. Biochemistry 41:1–7